

Query Details

[Back to Main Page](#)

1. Please check if article title is presented correctly. Otherwise, kindly amend.

2. Kindly check and confirm whether the corresponding author and if his/her email address is correctly identified and presented correctly.

Yes, updated

3. Please check and confirm if the authors and their respective affiliations are correctly identified and amend if necessary.

Yes, checked

4. Please check if sections and subsections are properly captured and presented and check if the section headings are assigned to appropriate levels.

Yes Checked

5. Please check and confirm if authors' emails are assigned to the appropriate author. Otherwise, kindly amend.

yes

6. Please confirm if the author names are presented accurately and in the correct sequence (given name, middle name/initial, family name). Author 1 Given name: [specify authors given name] Last name [specify authors last name]. Also, kindly confirm the details in the metadata are correct.

Yes, Checed

7. Please check if figures and captions are captured/presented correctly.

perfect

8. Please check all equations if captured and presented correctly.

yes, correct

9. A citation for Table 1 was inserted here so that table citations are in sequential order. Please check if appropriate. Otherwise, insert citation(s) in sequential order.

Good, thank you

10. Please check Tables 1 and 2 if presented correctly.

yes, correct

11. Please check and confirm if back matter sections and statements are captured correctly. Otherwise, kindly amend

yes

12. Please provide complete bibliographic details of this references [2, 4, 5, 6, 14, 15]

Updated

RESEARCH

Climate Change Impact on Geographical Region and Healthcare Analysis Using Deep Learning Algorithms

Springer Nature or its licensor (e.g. a society or other partner) holds exclusive rights to this article under a publishing agreement with the author(s) or other rightsholder(s); author self-archiving of the accepted manuscript version of this article is solely governed by the terms of such publishing agreement and applicable law.

[Ganduri Srikanth](#) 

Email : srikanth.ganduri6@outlook.com

[Affiliationids : Aff1, Correspondingaffiliationid : Aff1](#)

[Ch V. Raghavendran](#)

Email : raghuchv@yahoo.com

Affiliationids : Aff2

M. Ramkumar Prabhu

Email : ramkumarprabhu@gmail.com

Affiliationids : Aff3

Marepalli Radha

Email : marepalli.radha@gmail.com

Affiliationids : Aff4

N. V. Siva Kumari

Email : pnvskumar@kluniversity.in

Affiliationids : Aff1

Sabitha Kumari Francis

Email : sabithaamar@gmail.com

Affiliationids : Aff5

Aff1 Department of English, Koneru Lakshmaiah Education Foundation, Vaddeswaram, Andhra Pradesh, India

Aff2 Department of IT, Aditya College of Engineering and Technology, Surampalem, India

Aff3 Department of ECE, Saveetha School of Engineering, Saveetha Institute of Medical and Technical Sciences, Tamil Nadu, Chennai, India

Aff4 Department of CSE, CVR College of Engineering, Hyderabad, Telangana, India

Aff5 Department of English, Malla Reddy Engineering College, Secunderabad, Telangana, India

Received: 16 September 2024 / Revised: 7 December 2024 / Accepted: 18 December 2024

Abstract

AQ1 Climate change is a worldwide concern that needs to be taken into account and handled right away. On adaptation and mitigation of climate change, numerous articles are published. To investigate intricacies of climate change as well as **AQ2** develop more effective and economical policies for reduction and adaptation, new approaches are necessary. Climate change is one of the many domains where machine learning (ML) and deep learning (DL) methods have become **AQ3** increasingly prominent as a result of technological advancements. This research proposes a novel method in climate change impact in geographical region analysis and its healthcare training using deep learning model. Here, the input is **AQ4** gathered as a climatic analysis based on geographical change, and it is then processed for noise reduction, normalization, and smoothing. Processed data features are extracted and classified using region mask Gaussian component **AQ5** modeling with adversarial convolutional Boltzmann neural networks. The attributes that were retrieved display a climate change-based analysis of healthcare data. Experimental analysis is carried out in terms of training accuracy, specificity, recall, *F*-measure, and ROC. The proposed approach yielded 97% training accuracy, 93% recall, 90% ROC, *F*-measure of 92%, and 95% specificity. **AQ6**

Keywords

Climate change
Machine learning (ML)
Deep learning (DL)
Geographical region analysis
Climatic analysis
Adversarial convolutional Boltzmann neural networks

1. Introduction

Global population trends are already showing the consequences of climate change on health, and these trends pose a threat to past 50 years of progress made in public health worldwide. Direct effects of heat as well as extreme weather events, ecosystem-mediated effects, and effects mediated by socioeconomic pathways are just a few of the causal pathways through which changing climate can affect health. Additionally, it is anticipated that climate change may erode coping mechanisms, particularly in low-income areas [1]. A prompt and ongoing evaluation of the body of scientific knowledge serves as the foundation for identifying the most important connections between health and climate change, which will allow for adaptation and mitigation measures that promote health. The availability of such evidence evaluations is limited by two criteria. First, research on relationship between climate change and health is conducted in a variety of disciplines and silos, creating a fragmented landscape of specialized discourses that makes it difficult to synthesize important findings and spot patterns and gaps in the available data. Second, traditional evidence synthesis techniques—which usually need significant human resources to manually compile and screen literature—are no longer adequate or practical due to the exponential growth of available literature [2]. In fact, many evidence syntheses have responded to this conundrum by reducing the scope of their reviews, looking at a smaller and smaller percentage of the literature, and jeopardizing the possibility of gaining deeper understanding across disciplinary boundaries. Long-term, substantial changes in meteorological parameters including temperature, precipitation, wind direction, and speed within the earth's climate system are referred to as global climate change. This shift affects many Earthly systems, such as atmosphere, seas, glaciers, terrestrial ecosystems, and human cultures, it occurs over decades or even millions of years [3]. One of the most important

environmental concerns facing world today is global climate change, which has far-reaching effects on biodiversity loss, natural environment changes, an increase in extreme weather events, and numerous obstacles to social and economic advancement on a worldwide scale. In recent years, use of ML algorithms to predict climate change has become a focus for research. Predicting global climate change is a very complex and diverse field of study. Beginning in late 1970s of twentieth century, World Meteorological Organization, United Nations Environment Programme, and International Association of Hydrological Sciences all worked together to promote study on effects of climate change. Hydrological as well as climatic communities, both domestically and internationally, have long been interested in effects of climate change on water supplies as well as hydrology [4]. Using ML approaches has proven to be a useful tool for realising and anticipating climate-related challenges, as the topic of climate change is exceedingly complicated and requires multidisciplinary research. ML is broadly divided into two groups: supervised and unsupervised. The purpose of supervised approaches is to identify meaningful patterns from data and connections to unknown inputs. They rely on an a priori specification of a response variable and link inputs to system outputs. Finding new linkages, or teleconnections, between various facets of climate models may be facilitated by unsupervised learning [5].

2. Literature Review

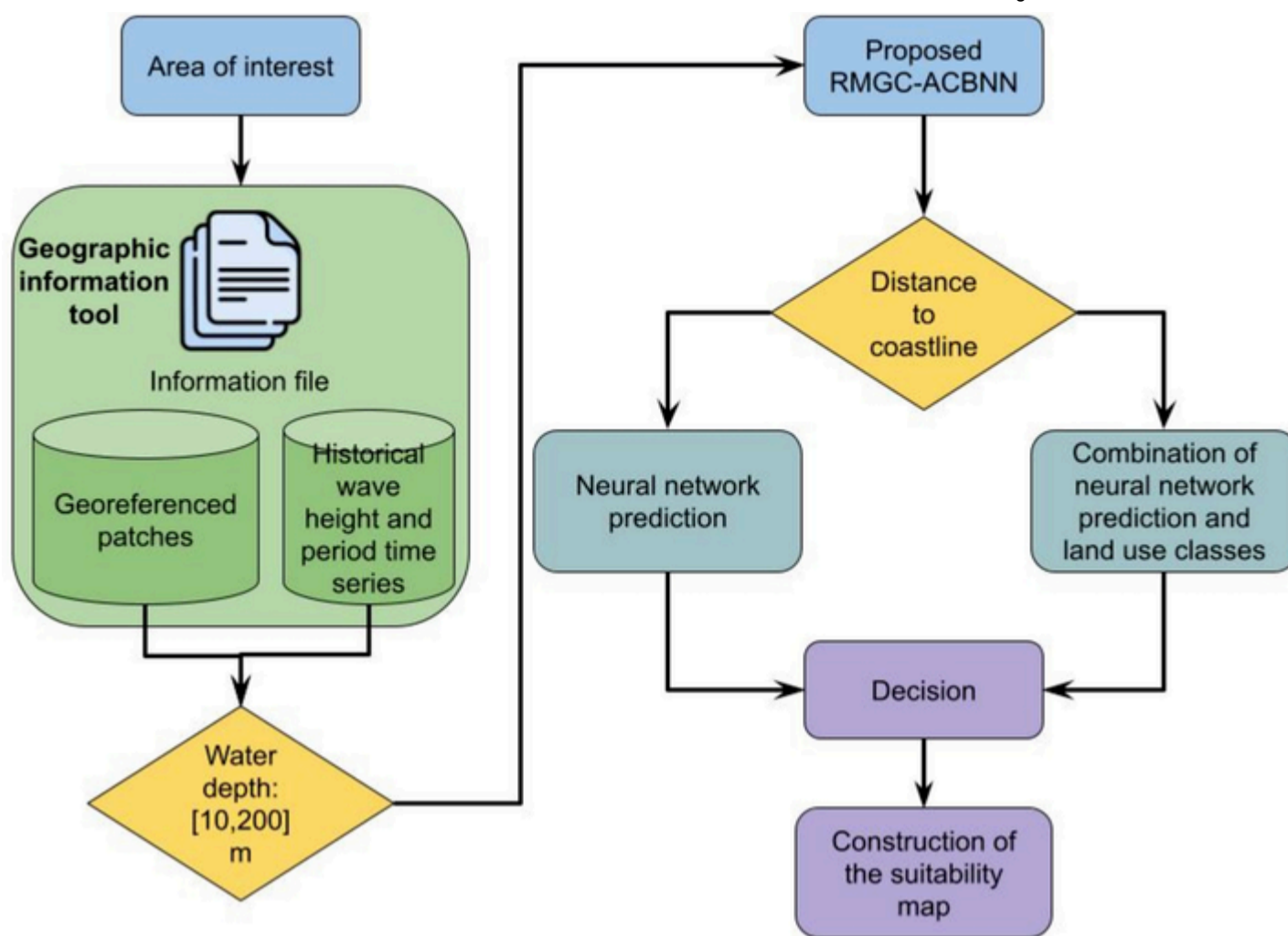
Geological and environmental variables are the two main categories into which landslide-related problems can be classified, according to previous studies. Lithology, elevation, slope, aspect, and curvature are examples of static, or comparatively unchanging, geological characteristics. Environmental variables, such as LULC and distance to the road, are dynamic since they vary annually; LULC is one example of this [6]. Effects of various LULC types on landslides vary. Prior research has demonstrated that human activities, especially in hilly areas, can raise the incidence and intensity of landslides [7]. Large-scale deforestation can accelerate the rate at which heavy rains induce erosion, which can lead to landslides. Mask R-CNN-based instance segmentation for water body recognition from satellite images is demonstrated in a recent research work [8]. The goal of this kind of research for automated flood monitoring has been covered by the writers. Additionally, a novel method called CO-attention Siamese Network (COSNet) has been presented in study [9] to tackle the object segmentation challenge. The authors have once more suggested object segmentation using episodic graph memory networks in [10]. Nonetheless, non-areal objects in movies, most human actions, and other contexts are the main emphasis of both publications. The authors of [11] have put forth YOLACT, a real-time segmentation network. Additionally, the same authors released YOLACT + +, an enhanced version of the program, the following year [12]. These variations are, however, slower in frames per second but less precise than the commonly used Mask R-CNN. On the other hand, deep neural networks are networks that have a large number of intermediary layers and are capable of learning to identify abstract concepts such as lines, geometric structures, and even whole scenes [13]. ANNs can produce continuous numbers or the certainty that an input belongs to a specific data class, even when they are trained on nonlinear functions. But as is noted, this confidence is not always equal to the frequentist probability of the prognosis being accurate [14]. Consequently, classifiers—models that distinguish between discrete categories—and regression models—models that infer continuous values—can be created using such networks. Since feedforward operations alone cannot enable the network to learn and generalize to new input, most ANN applications rely on this capability [15].

3. Proposed Climate Change Impact in Geographical Region Analysis and Its Healthcare Training

Within the network's top layer, we nest linear-in-parameters regression requirements that we took from the literature on yield and climate modelling (Fig. 1). This enhances efficiency and eventually performance above fully nonparametric neural networks and both existing parametric approaches, when used with a range of complementing techniques covered below. The distinction lies in the fact that it obtains distinct masks for a single input image by utilizing several backbone networks. Subsequently, the mask is combined using either pixel-wise intersection or union. It has been noted that the pipeline works better for assessing a water body's yearly form changes.

Fig. 1

AQ7 Proposed climate change impact in geographical region analysis



4. Region Mask Gaussian Component Modeling with Adversarial Convolutional Boltzmann Neural Networks (RMGC-ACBNN)

The research employed a supervised categorization method, which facilitates the creation of a themed map and eases information interpretation. Unlike unsupervised approaches, this approach necessitates threshold selection or data training. Of the total data, 75% is used for network training and 25% is used for testing. Here, 112 * 112 is used because the network input size for the test and training data must be the same. Data and labels are supplied to the deep neural networks as input to help them get trained. Fine-tuning has been used to speed up training and lower the number of calculations. As a result, the training function's accuracy rises and the model ought to receive better training. The test data are analyzed since the change detection model's final evaluation determines that the data are well-trained. At this stage, the output from the earlier sections is examined to see if it was correctly trained. If not, it can then be sent back to the network's training portion for more training, parameter optimization through adjustment of the learning rate, and setting and repetition of the designated procedures. Finally, the change detection final map is produced.

The covariance matrix, mean vector, and mixing weight are the three parameters of a GMM. New symbols were assigned to these parameters, which are as follows by Eq. 1: A Q8

$$(a_i, \mu_i, \Sigma_i), i = 1, 2, \dots, V \quad 1$$

where V is number of Gaussian distributions, Σ_i is the covariance matrix, μ_i is mean vector, and a_i is mixing weight. If a set of points in d -dimensional space is given by $x_n, n = 1, \dots, N$, then probability density function of points can be expressed as Gaussian frequency function $g(x_n; \mu_i, \Sigma_i)$ by Eq. 2:

$$g(x_n; \mu_i, \Sigma_i) = \frac{1}{\sqrt{(2\pi)^d |\Sigma_i|}} \exp \left[-\frac{1}{2} (x_n - \mu_i)^T \Sigma_i^{-1} (x_n - \mu_i) \right]$$

$$p(x_n; \mu_i, \Sigma_i) = \prod_{i=1}^n g(x_n; \mu_i, \Sigma_i) \quad 2$$

where the probability density is denoted by $g(x_n; \mu_i, \Sigma_i)$. Principal components are the name given to eigenvectors. They first undergo a standard normalization because of the different feature domains. In the extraction task, the aforementioned eigenvectors produce a covariance matrix. If λ_i is an eigenvalue p of this eigenvector, following equation can be utilized to determine percentage of the total variance that comes from the r of the initial vectors by Eq. 3:

$$\lambda = \frac{\sum_{i=1}^r \lambda_i}{\sum_{i=1}^r \lambda_i + \sum_{r+1}^p \lambda_{r+1}} \quad 3$$

Because the central limit theorem predicts that random integers joined together will have a Gaussian distribution. As a result, we considered the null hypothesis, which states that $u \mp i$ obeys the Gaussian distribution. As can be seen in the example below, it performed well. A steep peak at $1 - P_i \sim 1$ indicates is to be selected, and the histogram of $1 - P_i$ should be flat when it obeys the null hypothesis. The maximizing of standard deviation of $h_n(1 - P_i) \in R104$ for microarrays, $R103$ for HTS, $n < n_0$, where h_n is n th histogram, n_0 is biggest n that meets condition of adjusted $P_i(\in h_n)$ greater than P_0 , a threshold adjusted p -value, is how $\sigma \ell$ is optimized.

With W in width and W in height, window size of this cube encircling a pixel is $W \times$. Given that the spectral bands have N channels, size of the entire cube is $W \times W \times N$. In order to classify data, our network will employ fusion and dual-channel blocks. The dual-channel block will compress the cube to the proper size after learning the spectral and spatial information surrounding the label pixel. The fusion block uses the dual-channel block's output as its input to do the final classification after learning the input. To increase the categorisation

accuracy, a generator is employed to create a cube of the same size. The generator enhances the classification outcomes in the ablation trials. Input cube is divided into M groups with a dimension of $W \times W \times N$. Every group has p pixels for both width and height, where $W/p = M = (W/p)2M$.

By producing high-quality samples, G hopes to fool D and increase the likelihood that DD will make a mistake, whereas D seeks to distinguish between created samples (z) $G(z)$ and genuine samples x as accurately as possible. By locating the Nash equilibrium between G and D , the optimization of GAN is achieved. Value function $(D, V(D, G))$ optimizes G and D by Eq. 4:

$$\min_G \max_D V(D, G) = E_{x \sim p_{\text{data}}(x)} [\log D(x)] + E_{z \sim p_z(z)} [\log(1 - D(G(z)))] \quad 4$$

Generator aims to maximize probability that discriminator will classify generated samples as true classes. Generator features a novel combined spatial-spectral hard attention model that protects significant features along the spatial and spectral dimensions while suppressing less significant elements. It enhances the features by employing an adaptive spatial-spectral attention map. This attention map is based on a multi-branch convolutional network and is created utilizing dynamic activation function and an element-wise subtraction operation. Each generator transposed convolutional layer is preceded by the addition of spatial-spectral hard attention module. Simultaneously, it gives different consideration to spectral and spatial contextual factors. Following adaptive feature selection, characteristics of the generated samples whose distribution closely resembles distribution of the actual sample are kept, while the confusing and deceptive features are removed.

Let $I \in RH \times W \times B$ represent HSI, where H , W , and B stand for spectral signatures' respective band number, spatial height, and spatial breadth. I is first processed for data preparation in order to obtain the spectral-spatial information from it. Every i in I creates a fixed square box, with i serving as center pixel and a given number of surrounding pixels serving as adjacent pixels. Consequently, the HSI ultimately produces an overall quantity of HW cubes, signifying a sample set $I = \{I_1, I_2, \dots, I_{HW}\}$. In this case, the sample of pixel i is denoted by $i \in RS \times S \times B$, and the spatial size is indicated by $S \times S$. The associated labels of I are represented by the label set $y = \{y_1, y_2, \dots, y_{HW}\}$, where n is total number of classes of ground truth and $y_i \in \{1, 2, \dots, n\}$ is center pixel of each sample. In the second section, spectral-spatial properties are extracted by feeding the samples into CNN. The convolutional layer, maxpooling layer, leaky-ReLU operation, and fully connected (FC) layer are some of layers that make up the CNN. The most important component among them is the convolutional layer, which is best explained as follows by Eq. 6:

$$f_{ij}^{xy} = \sum_o \sum_{p=1}^r \sum_{q=1}^s w_{ijm}^{qt} f_{(i-1)m}^{(x+q)(y+1)} + b_{ij} \quad 5$$

where x and y stand for respective positions in feature map, r and s are kernel sizes, q and t are kernel indices, m is feature map index, and b is bias. Output variable in j th feature map at i th layer is indicated by expression f_{ij}^{xy} . We commonly choose pertinent spectral bands and subsequently enhance the classification by using entropy measures like H , MI, or KLD. While choosing different spectral bands can be achieved with KLD, informative spectral bands (with high entropy) can be preserved when band selection is done with H . As a result, we suggest using both H and KLD to automatically choose spectral bands that are both informative and unnecessary. Formally, given an HSI $X = [\times 1, \dots, x_N] \in R N \times D$, where D is number of all spectral bands, N is number of pixels, $x_i, i \in \{1, 2, \dots, N\}$, denotes a spectral vector of a pixel. Thus, the goal of the suggested unsupervised band selection approach is to choose a smaller number, d , from each spectrum band, such that $d \geq D$.

It accomplishes a layer-by-layer training process that fine-tunes with needed data and trains the unlabelled data. In contrast to deep convolutional network and deep belief network, interference procedure adds top-down feedback to bottom-up process, enabling DPM to more effectively account for ambiguity regarding unclear inputs. Additionally, it optimises the layers with an approximate variational lower bound gradient. This introduces an improved generative facilitative learning model. To pretrain a deep Boltzmann machine (DBM) with three hidden layers, one must first learn a stack of RBMs, which are then combined to form the DBM. to define the energy function of the DBM in order to make its structure more clear. For the 2-layer method as described in Eq. 7.

$$E_{DBM}(v, h^{(1)}, h^{(2)}; \theta) = -v^T W h^{(1)} - h^{(1)T} v h^{(2)} - d^{(1)T} h^{(1)} - d^{(2)T} h^{(2)} - b^T v \quad 6$$

Equations 5 and 6 are obtained by increasing the lower bound while paying respect to the mean-field distribution. These equations are then repeated until convergence is achieved. $-h \cdot v T$ is the derivation of the gradient's first part. Nevertheless, computing the gradient's second part is once more challenging. We estimate it using the Gibbs sampling approach in order to address this problem. We can sample values ht from the hidden layer using input vt , as shown in Eq. 4. Then, using Eq. 5, we can sample a new vector $v_0 t$ on the visible layer once more given the vector ht . We obtain a random sample from the provided distribution after doing this k times. It can be demonstrated that $-h(k) t \cdot v(k) T t$ is a reasonable approximation for the negative portion of the gradient. In actuality, $k = 1$ alone can produce satisfactory results. Lastly, the algorithm's update rule can be expressed as follows in Eq. 8:

$$w_{t+1} = w_t + \alpha (h_t \cdot v_t^T - h'_t \cdot v_t^T) \quad 7$$

where learning rate (α) is expressed. In a similar manner, the updating rules for biases can be obtained, as shown by Eqs. 9 and 10:

$$a_{t+1} = a_t + \alpha (v_t^T - v_t'^T) \quad 8$$

$$b_{t+1} = b_t + \alpha (h_t^T - h_t'^T) \quad 9$$

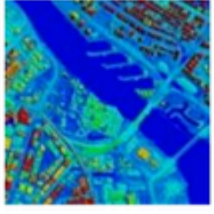
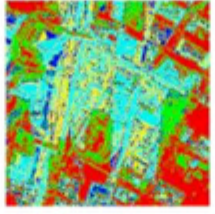
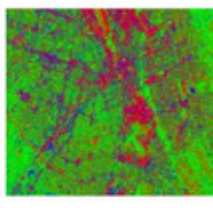
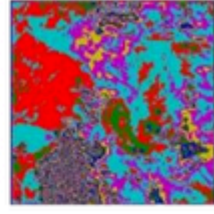
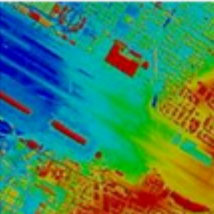
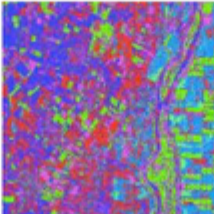
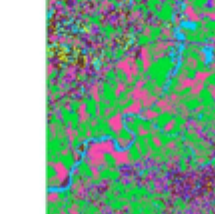
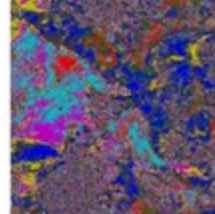
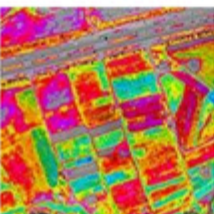
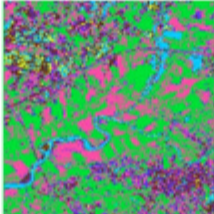
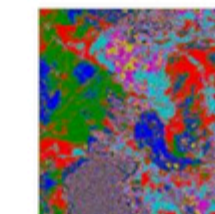
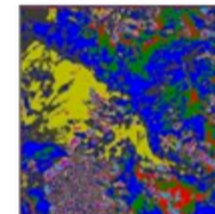
It can be improved even more by including solutions common to several other well-liked learning techniques, including gradient momentum or learning rate decay, which may facilitate learning.

5. Results and Discussion

Our system is compared with continuous variable mapping benchmarks in a simulated environment. Simulations, which simulated a synthetic data gathering problem in a $30 \text{ m} \times 30 \text{ m}$ zone, were carried out in Python on a single desktop computer with a 1.8-GHz Intel i7 processor and 16 GB of RAM. AQ9 (Table 1)

Table 1 AQ10

Comparative analysis in geographical image training for various datasets

Dataset	Geographical input image	CNN	DANN	RMGC-ACBNN
Bern Dataset				
San Francisco Dataset				
Farmland Dataset				

5.1. Dataset

- **Bern Dataset:** pixel size of image: 301×301 data source: satellite SAR sensor ERS-2; filming dates: April and May of 1999; scenario: the Bern airport and the entirety of the cities of Thun and Bern were inundated by the River Aare. open source: Yolalala/RS-source on Github
- **San Francisco Dataset:** pixel size of the image: 256×256 ; data source: satellite SAR sensor ERS-2 August 2003 and May 2004 were the shooting times. Situation: a developed area extending over the United States city of San Francisco, located at coordinates $37^\circ 28' N$, $121^\circ 58' W$. Open source: Yolalala/RS-source on Github
- **Farmland Dataset:** pixel size of the image: 257×289 Radarsat-2 satellite SAR sensor is the data sensor. Dates of shooting: June 18, 2008, and June 19, 2009 Situation: A result of recently planted regions near China's Yellow River Estuary. Single-look and four-look multi-temporal images, which are impacted by noises at varied intensities, are the corresponding types of images.

Table 2 above presents a comparative comparison of training of climate changes in satellite images for different input datasets. Based on the image training used to distinguish the land surfaces from the gathered satellite image, a comparison has been made. The suggested RMGC-ACBNN based training method has produced the most refined and improved results when assessing the input satellite image when compared to all other methods mentioned above.

Table 2

Comparative based on climate change impact in geographical region analysis

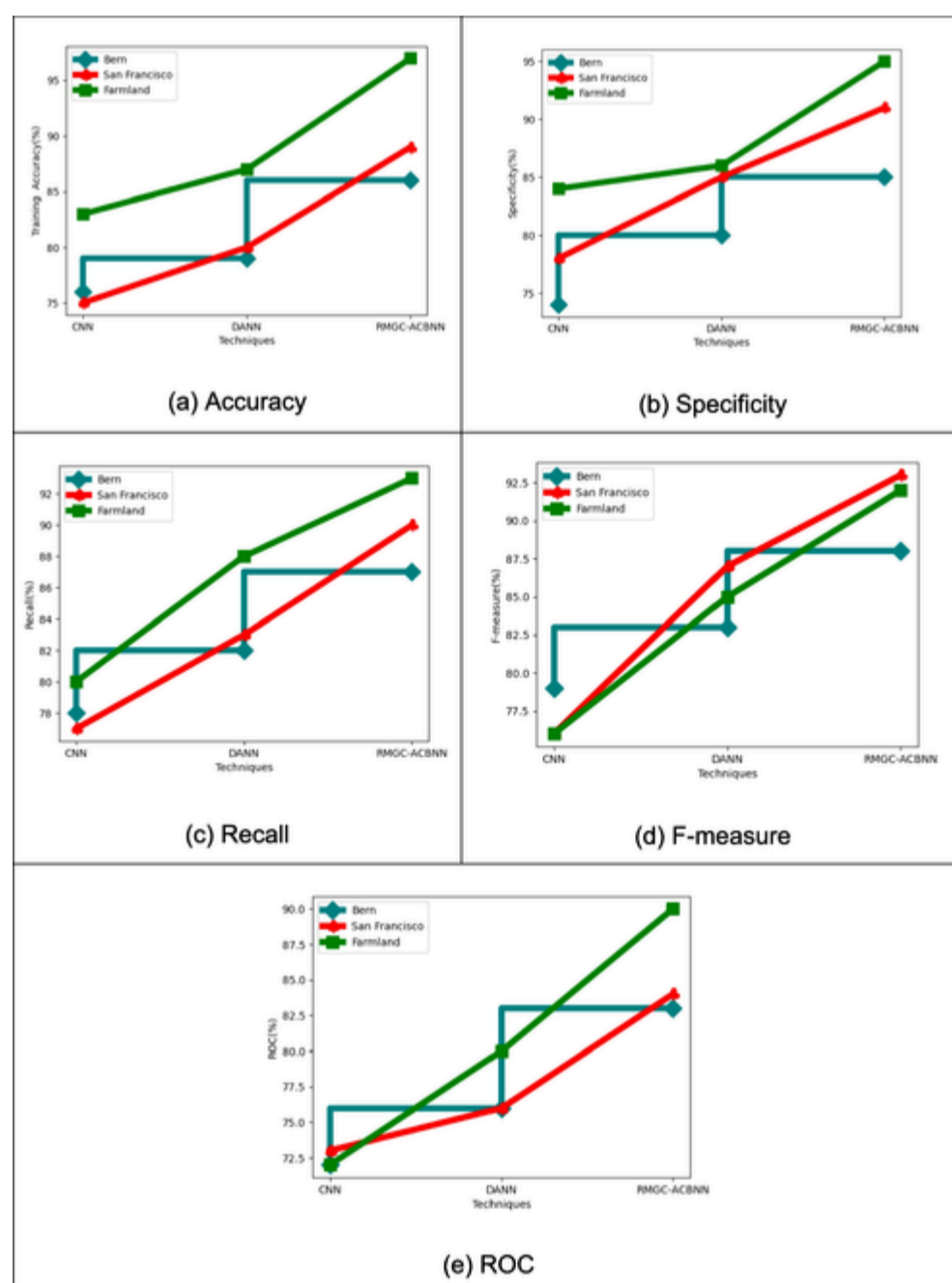
Datasets	Techniques	Training accuracy	Recall	Specificity	F-measure	ROC
Bern dataset	CNN	76	78	74	79	72
	DANN	79	82	80	83	76
	RMGC-ACBNN	86	87	85	88	83
San Francisco dataset	CNN	75	77	78	76	73
	DANN	80	83	85	87	76
	RMGC-ACBNN	89	90	91	93	84
Farmland dataset	CNN	83	80	84	76	72
	DANN	87	88	86	85	80
	RMGC-ACBNN	97	93	95	92	90

Table 1 above compares the suggested and current techniques with respect to dataset and parametric analysis based on climate change impact in geographical region analysis. Three different datasets—the Farmland, San Francisco, and Bern datasets—have been compared. Below is a graphical illustration of it. An R^2 of 0.924, a p -value of less than 0.001, and a standard error of 0.002 were obtained from the training runs. While the validation yielded a lower R^2 (0.305), probably because the model could not predict visitor values that aligned with the estimates provided by Flickr data, it is still capable of accurately predicting general geographic and magnitudinal trends in recreational ecosystem services. The empirical and modeled PUD's spatial association is confirmed by a computed Pearson correlation coefficient of 0.94.

The proposed and current techniques for climate change impact in geographical region analysis dataset are compared in Fig. 2 a–d. The recommended approach in this instance produced training accuracy of 86%, recall of 87%, ROC of 83%, F -measure of 88%, and specificity of 85%. For the Bern dataset, CNN achieved 76% training accuracy, 78% recall, 72% ROC, F -measure of 79%, and 74% specificity, in contrast to the prior DANN, which achieved 79% training accuracy, 82% recall, 76% ROC, F -measure of 83%, and 80% specificity. Then, 89% training accuracy, 90% recall, 84% ROC, F -measure of 93%, and 91% specificity were the outcomes of the recommended approach. The CNN obtained 75% training accuracy, 77% recall, 73% ROC, F -measure of 76%, and 78% specificity on the San Francisco dataset. With training accuracy of 80%, recall of 83%, ROC of 76%, F -measure of 85% and specificity of 87%, the current CNN performed well. For the Farmland dataset, the recommended approach yielded 97% training accuracy, 93% recall, 90% ROC, F -measure of 92%, and 95% specificity. The CNN obtained 83% training accuracy, 80% recall, 72% ROC, F -measure of 76%, and 84% specificity, while the current DANN earned 87% training accuracy, 88% recall, 80% ROC, F -measure of 85%, and 86% specificity.

Fig. 2

Comparison of parameters for climate change impact in geographical region analysis: **a** training accuracy, **b** specificity, **c** recall, **d** F -measure and **e** ROC



For regions with above-average recreation and below-average recreation, we evaluated the associated land cover class. It should come as no surprise that most summertime recreation took place in forests, with below-average activities taking place in shrublands. Our model predictions indicate that this pattern will continue into the future. In general, the amount of land that may be used for recreation decreases dramatically as a result of climate change. Prediction accuracy, which indicates the percentage of accurate predictions a model makes, is a fundamental and understandable assessment statistic used to assess a predictive model's performance. It is appropriate for class-balanced datasets and is simple to comprehend and apply, but it is misleading when dealing with datasets that include class-unbalanced datasets since it does not accurately reflect prediction performance of various classes. Therefore, in real-world applications, particularly in cases where the distribution of data types is not uniform.

6. Conclusion

In this study, a novel deep learning model for healthcare training and the investigation of the impact of climate change on geographic regions is proposed. This climate study is based on geographical change, and the information is gathered, processed, and normalized for noise reduction, smoothing, and normalization. Gaussian component modeling with region mask and adversarial convolutional Boltzmann

neural networks have been used to extract and classify the features from the processed data. Health data analysis based on climate change is displayed in extracted features. The created model can recognize the spatial constraints in satellite pictures, including constantly changing characteristics such as patterns of algae. In addition, the system treats the wave energy potential as a dynamic phenomenon with unpredictable temporal variability in order to evaluate it simultaneously. Furthermore, our model is able to distinguish between the variations in temporal variability of different places. Thus, the effectiveness of combining diverse data to solve complicated problems is proved. This development gives scientists a powerful tool to investigate the complex systems underlying climate change and to improve their projections, leading to improved readiness and reaction plans. Combination of climate science with machine learning improves forecast results while expanding the field of climate research. This collaborative approach holds great potential to advance our knowledge and adaptation tactics related to climate change on a worldwide scale, serving as a crucial first step towards more scientifically based environmental policy and planning decisions.

Publisher's Note

Springer Nature remains neutral with regard to jurisdictional claims in published maps and institutional affiliations.

AQ11 Author Contribution

Ganduri Srikanth: conceptualization, methodology, formal analysis, validation, resources, supervision, writing—original draft, and writing—review and editing. Ch V Raghavendran: validation, resources, supervision, writing—original draft, and writing—review and editing. M. Ramkumar Prabhu: formal analysis, validation, resources, writing—original draft, and writing—review and editing. Marepalli Radha: formal analysis, validation, resources, supervision, writing—original draft, and writing—review and editing. N. V. Siva Kumari: writing—original draft and writing—review and editing. Sabitha Kumari Francis: writing—original draft and writing—review and editing.

Data Availability

No datasets were generated or analyzed during the current study.

Declarations

Conflict of Interest

The authors declare no competing interests.

References

- Wang H, Li Y, Huang G, Ma Y, Zhang Q, Li Y (2024) Analyzing variation of water inflow to inland lakes under climate change: integrating deep learning and time series data mining. *Environ Res* 259:119478
- Durairaj, M., Rubenraju, K., Krishna, B.V.R. et al. Sustainable Agriculture-Based Climate Change Training Models using Remote Hyperspectral Image with Machine Learning Model. *Remote Sens Earth Syst Sci* 7, 261–270 (2024). <https://doi.org/10.1007/s41976-024-00118-y> AQ12
- Bai T, Wang L, Yin D, Sun K, Chen Y, Li W, Li D (2023) Deep learning for change detection in remote sensing: a review. *Geo-spatial Inf Sci* 26(3):262–288
- R. Hänsch and M. A. Chaurasia, "Earth Observation and Machine Learning for Climate Change," IGARSS 2024 - 2024 IEEE International Geoscience and Remote Sensing Symposium, Athens, Greece, 2024, pp. 1676-1682, doi: 10.1109/IGARSS53475.2024.10642282.
- Viet Du, Q. V., Nguyen, H. D., Pham, V. T., Nguyen, C. H., Nguyen, Q. H., Bui, Q. T., ... Petrisor, A. I. (2023). Deep learning to assess the effects of land use/land cover and climate change on landslide susceptibility in the Tra Khuc river basin of Vietnam. *Geocarto International*, 38(1). <https://doi.org/10.1080/10106049.2023.2172218>
- T. S. Balakrishnan, P. Krishnan, U. S. Ebenezar, M. Mohammed Nizarudeen and N. Kamal, "Machine Learning for Climate Change Impact Assessment and Adaptation Planning," 2024 International Conference on Trends in Quantum Computing and Emerging Business Technologies, Pune, India, 2024, pp. 1-6, doi: 10.1109/TQCEBT59414.2024.10545291.
- Hernanz A, Correa C, Sánchez-Perrino JC, Prieto-Rico I, Rodríguez-Guisado E, Domínguez M, Rodríguez-Camino E (2024) On the limitations of deep learning for statistical downscaling of climate change projections: the transferability and the extrapolation issues. *Atmos Sci Lett* 25(2):e1195
- Secci D, Tanda MG, D'Oria M, Todaro V (2023) Artificial intelligence models to evaluate the impact of climate change on groundwater resources. *J Hydrol* 627:130359
- Khan MI, Sarkar S, and Maity R (2023) Artificial intelligence/machine learning techniques in hydroclimatology: a demonstration of deep learning for future assessment of stream flow under climate change. In *Visualization techniques for climate change with machine learning and artificial intelligence* (pp. 247–273). Elsevier

10. Sujanthi S, Santhosh P, Raj MV, and Vishwa GP (2024). Climate change adaptation and mitigation using deep learning for urban environments. In 2024 2nd International Conference on Intelligent Data Communication Technologies and Internet of Things (IDCIoT) (pp. 1468–1473). IEEE
11. Gerges F, Boufadel MC, Bou-Zeid E, Nassif H, Wang JT (2024) Downscaling daily wind speed with Bayesian deep learning for climate monitoring. *Int J Data Sci Analytics* 17(4):411–424
12. Lagpong NNM, Ngono JM, Ele P, Noumsi V, Rudant JP, and Moffo FM (2023) Evaluation of machine learning and deep learning algorithms applied to earth observation data for change detection in polarimetric radar images. In *International Conference on Safe, Secure, Ethical, Responsible Technologies and Emerging Applications* (pp. 345–358). Cham: Springer Nature Switzerland
13. Nourani V, Tapeh AHG, Khodkar K, Huang JJ (2023) Assessing long-term climate change impact on spatiotemporal changes of groundwater level using autoregressive-based and ensemble machine learning models. *J Environ Manage* 336:117653
14. Srivastava, S., Ahmed, T. DLCD: Deep learning-based change detection approach to monitor deforestation. *SIViP* 18 (Suppl 1), 167–181 (2024). <https://doi.org/10.1007/s11760-024-03140-1>
15. Deep, G., Verma, J. (2024). Deep Learning Models for Fine-Scale Climate Change Prediction: Enhancing Spatial and Temporal Resolution Using AI. In: Tripathi, G., Shakya, A., Kanga, S., Singh, S.K., Rai, P.K. (eds) *Big Data, Artificial Intelligence, and Data Analytics in Climate Change Research*. *Advances in Geographical and Environmental Sciences*. Springer, Singapore. https://doi.org/10.1007/978-981-97-1685-2_5